Growing Profile Monitoring with Dynamic Time Warping Alignment

Chenxu Dai[1], Kaibo Wang[1*] and Ran Jin[2]

[1:] Department of Industrial Engineering, Tsinghua University, Beijing 100084, China

[2:] Grado Department of Industrial and Systems Engineering, Virginia Tech., VA 24061, USA

Abstract

In conventional profile monitoring problems, profiles for different products or process runs are assumed to have the same length. Statistical monitoring cannot be implemented until the whole profiles are obtained. However, in some cases, a profile should be monitored when it growth with time, so that the root causes can be identified and automatic compensations can be initiated as early as possible. Motivated by an ingot growth process in semiconductor manufacturing, we propose a monitoring method for growing profiles with unequal lengths and time-varying means. The profiles are firstly aligned by using dynamic time warping (DTW) algorithm, and then averaged to generate a baseline. Online monitoring is performed based on the incomplete growing profiles. Both simulation studies and a real example are used to demonstrate the performance of the proposed method.

Key Words*: dynamic time warping, profile monitoring, quality control, statistical process control*

[*] Corresponding author: Dr. Kaibo Wang, Department of Industrial Engineering, Tsinghua University, Beijing 100084, China. Email: kbwang@tsinghua.edu.cn. Tel.: +86-10-62797429

1 Introduction

Statistical process control (SPC) methods are extensively used to monitor and improve the quality and the productivity in manufacturing and service operations.[1] One important tool is the control chart, which is often set up to monitor the key process variables and to trigger alarms when abnormal changes are detected. In the literature, a collection of methods has been developed for processes with one variable or multiple correlated variables.[2] Recently, profile monitoring has received attentions.[3] A profile, which is shown in the form of a functional curve, illustrates the relationship between one response variable and one or more explanatory variables (e.g., time and locations).

If the profile can be fitted using a parametric model, the model parameters are usually used for process monitoring.[4,5] For example, to monitor a linear profile, Kang and Albin[6] fitted a simple linear regression model to the Phase I data and monitored all the parameters and the residual standard errors by using the T^2, exponentially weighted moving average (EWMA), and R charts. To monitor a more complex roundness profile, Colosimo *et al.*[7] proposed to fit a spatial autoregressive regression model, based on which a vector of parameters is estimated and used for statistical monitoring.

If the profile is too complicated to be characterized by any parametric form, nonparametric methods are sometimes employed. In nonparametric control charts for profiles, the charting statistic is usually developed based on the metrics that measure the departure of the observed profiles from a baseline.[3] Gardner *et al.*[8] designed several simple methods to calculate the departure metrics (e.g., the integral of squared differences). Jones and Rice[9] and Nomikos and MacGregor[10] proposed to monitor the scores of the principle components and the residuals obtained from principle components analysis (PCA). Jeong *et al.*[11] used wavelets to transform

high-frequency signals for process monitoring. Walker and Wright[12] demonstrated the use of spline models to fit and monitor complex profiles. Zou *et al.*[13] used nonparametric regression to fit a profile dataset. To filter out the rotation, translation, and isometric scaling (dilation) effects, Del Castillo and Colosimo[14] proposed a Generalized Procrustes Algorithm (GPA) to use the full Procrustes distances as the metrics after the profiles are registered or superimposed. Woodall *et al.*[3] presented a thorough literature review of related works on profile monitoring.

The conventional profile monitoring methods usually assume that the complete profile is available so that the charting statistics can be calculated. Thus, all observations on a profile are required to construct the control chart. However, in some manufacturing processes, a profile dynamically grows in production, where the faults should be detected once they occur in the middle of a production cycle. Thus, the root causes can be identified, and automatic compensations can be initiated as early as possible. This demands an online monitoring strategy based on the partially observable growing profiles.

Taking the ingot growth process as a motivating example, the ingot grows in a highly automatic furnace (shown in Table 1). In this production, raw polysilicon materials are melted in a quartz crucible with the temperature over 2000 F. A seed crystal is dipped into the silicon melt and pulled up slowly to induce the growth of the single crystal ingot. The cycle time to grow one ingot may take over 50 hours. In this process, all key process variables, such as pulling speed, temperature and heating power, must be perfectly coordinated to ensure desirable growth environment. Once the process becomes nonconforming, compensation actions need to be taken immediately to reduce the material and energy waste. Therefore, monitoring the key parameters online are of great importance for the ingot growth process to ensure quick change detection and quality loss prevention.

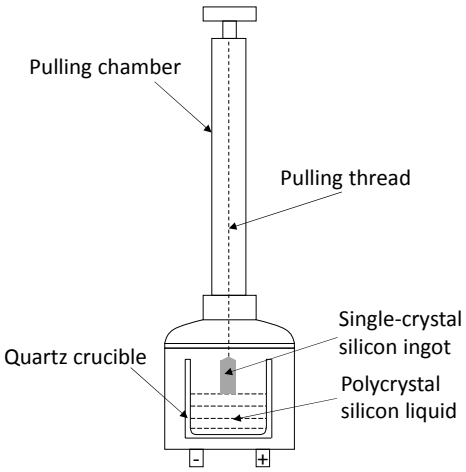

Figure 1. A schematic drawing of the single-crystal ingot growth furnace

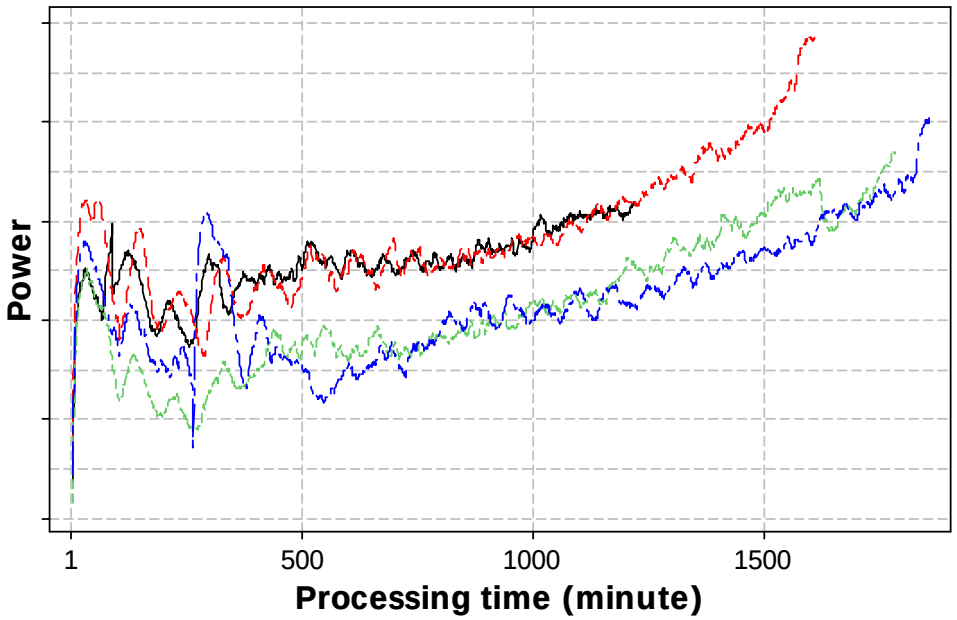

Figure 2. Examples of power profiles in the ingot growth process

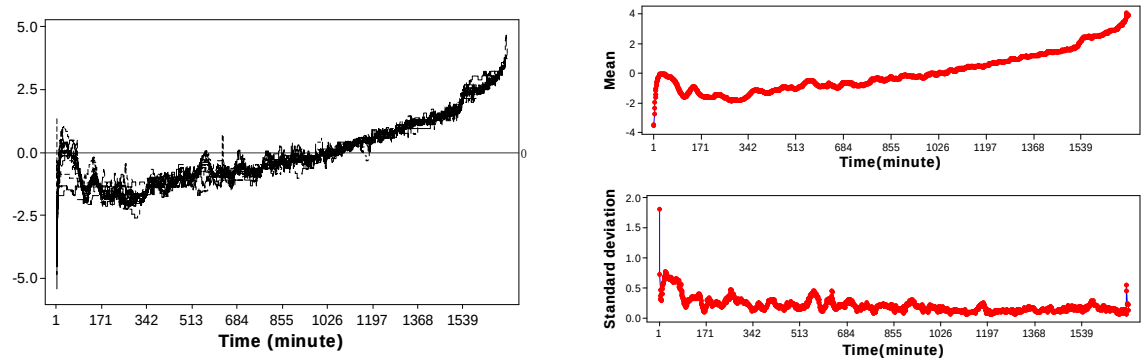

(a) (b)

Figure 3. Plots of aligned samples and their mean and standard deviation. (a) A collection of aligned samples. (b) The mean and standard deviation of the aligned samples.

In this study, we focus on the heating power profile, which is a key parameter in the process to affect ingot quality. Because of the complex growing mechanism, the power exhibits a dynamic profile in the growth cycle. Figure 2 shows four examples of power profiles collected during the ingot growth process. Each curve represents one growth cycle, which corresponds to the growth of one ingot. Figure 3 shows more aligned samples (the concept of profile alignment will be explained in a later section) and their mean and standard deviation curves. Compared with the profile data that are usually observed in the existing literature, the power profiles in Figure 2 have several unique features: (1) the profiles have a time-varying mean. The means of different profiles are not identical, and all profiles follow a similar variation pattern. The trend of the profiles is governed by the physical mechanism of the growth process. An upward or downward shift of the entire profile does not imply an engineering failure. Instead, a significant deviation from the mean trend indicates possible process changes that should be detected. (2) The profiles have different lengths. The cycle time of each growth run is determined by the amount of raw materials used. The more raw materials used, the longer cycle time is expected. Therefore, the length variation of profiles is treated as conforming in this process. (3) The profiles show large variations in the early stage of the production cycle and gradually stabilize when the process

evolves; that is, the inherent variation of the profile varies over time. (4) During the online monitoring, the profile will continue to prolong with time to an unknown limit. Although there are many observations of the profile when a production cycle finishes, the charting statistic must be evaluated using incomplete profiles online. This growing feature of the profiles makes the online monitoring problem unique.

The profile data collected from the ingot growth process convey important engineering knowledge about process failures. Given an in-control baseline profile, the deviation of an online profile from the baseline usually indicates an instant failure of the growth process, usually caused by growth process or raw materials. Then, the growth process must be stopped to reduce material and energy losses. The profile-to-profile variation represents slow or abrupt changes of equipment conditions. For example, the resistivity of the heater will become larger as more production runs are carried out, where the efficiency of the thermal field is gradually reduced with more production cycles. Therefore, practitioners must monitor this process and detect unexpected process shifts early.

It should be noted that the monitoring of the growing profile is different from the monitoring of a short-run process, which has been studied in the literature.[15] For a short-run process, the key is to start the chart as quickly as possible, because the process may terminate shortly. Therefore, self-starting charts are usually appropriate for such processes.[16] Moreover, the mean of an in-control short-run process is usually assumed to be a constant. However, in the ingot growth process, each complete growing profile usually contains thousands of data points, which is a data-rich process for monitoring. In addition, the mean of the growing profile changes over time.

Given the above unique features of the growing profiles, challenges such as the dynamic means, profile alignment, unequal variance and incomplete profiles must be addressed in the design of

the control chart. In this paper, we propose a method to monitor these unique growing profiles. More specifically, we propose to use a time-warping technique to align the raw profiles and build a baseline model; then, we use the generalized likelihood ratio for online monitoring based on the incomplete profile data.

The rest part of the paper is organized as follows. The details of the charting strategy are presented in Section 2. In Section 3, we study the performance of the proposed chart and compare it with a benchmark method in simulation studies. In Section 4, we further conduct a real case study in ingot growth processes to show the effectiveness of the proposed method. Finally, we conclude this paper with suggestions for future research in Section 5.

2 Profile monitoring based on dynamic time warping

To tackle the unique challenges in growing profile monitoring, we propose a framework based on dynamic time warping, as shown in Figure 4.

Starting with the historical profile samples, we will identify the in-control behavior of the variables. Therefore, profiles with different lengths and locations should be firstly aligned; then, a baseline profile is calculated, which serves as the in-control benchmark for online monitoring. During the online monitoring stage, each incomplete growing profile will be aligned with the in-control baseline; then, a charting statistic is evaluated. The alignment and monitoring will be repeated when a new observation of the profile becomes available for online monitoring.

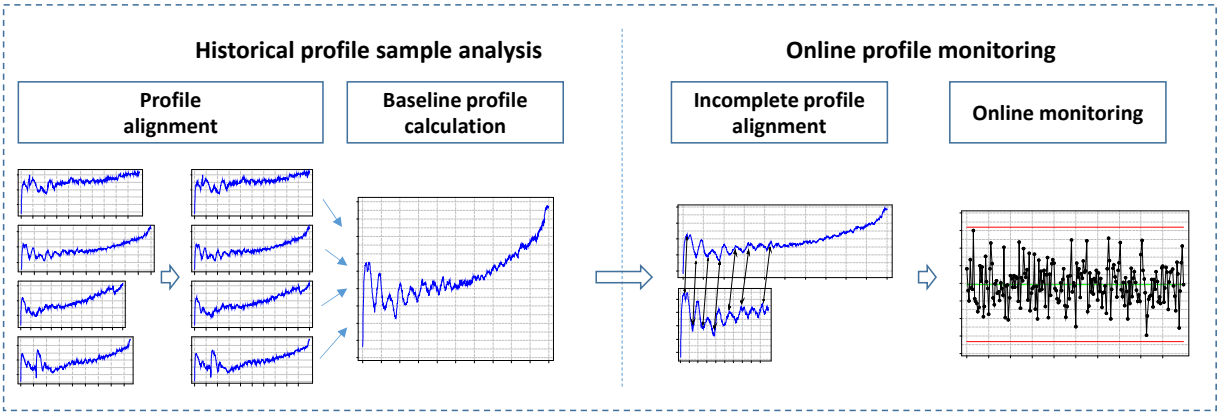

Figure 4. The framework for growing profile monitoring

2.1 Profile alignment

To construct a reliable baseline for online monitoring, all profiles must be aligned to have an equal length. Because of the engineering mechanism, all in-control profiles should exhibit a similar pattern. Thus, the alignment operation will use the similar patterns to stretch or compress different segments of a profile to match with another profile. The dynamic time warping (DTW) algorithm is suitable for this purpose.

DTW was first proposed in the context of speech recognition to account for the differences in speaking rates between speakers and utterances. The rationale behind DTW is that we can locally stretch or compress any two profiles to make one resemble the other as much as possible.[17,18] Gupta *et al.*[19] and Dai and Zhao[20] used dynamic time warping (DTW) for fault diagnosis. Kassidas *et al.*[21] used DTW to synchronize historical profiles and create a database of historical time-aligned in-control profiles, but they did not explain the methods for choosing a standard profile or how to monitor a new profile.

Denote any two profiles as X and Y with lengths L_X and L_Y respectively. DTW attempts to match one of the profiles (which is usually called the query) to the other profile (which is usually

called the reference), and to improve the similarity of their variation patterns. Let k, $k = 1, 2, ..., T$, be the time index of the aligned profile, and let $\phi_x(k) \in \{1, 2, ...L_X\}$ and $\phi_y(k) \in \{1, 2, ...L_Y\}$ be the remapped time indices of the query and the reference profiles, respectively. Let $d(\phi_x(k), \phi_y(k))$ be a distance measure between point $\phi_x(k)$ on X and point $\phi_y(k)$ on Y. Then, the best alignment is obtained by minimizing the total distance between these two profiles:

$$D(\mathrm{X}, \mathrm{Y}) = \min_{\phi} \sum_{k=1}^{T} d(\phi_x(\mathrm{k}), \phi_y(\mathrm{k})) \ . \qquad (1)$$

In practice, the Euclidian distance is commonly used. The distance function is minimized using a dynamic programming algorithm. The last segment on the query profile is matched to the reference profile according to a predefined step function. When the last segment is matched, the algorithm moves one step forward to continue this procedure until the entire profile is processed.

To account for the requirements raised by real problems, additional constraints should be jointly applied in the algorithm, including (1) the monotonicity constraint, which ensures that the data points on the query profile and those on the reference profiles have the same time sequence; (2) the symmetric continuity constraint, which ensures that all data points are mapped onto the reference profile and no points are missed; and (3) the start and end point constraint, which ensures the start and end points of the two profiles are exactly aligned. Some examples of DTW-aligned profiles are shown in Figure 5. The detailed algorithm of DTW is described in [18] and the references therein.

It should be noted that DTW is not invariant to location shifts of the profiles. Therefore, the mean of the profiles should be removed before alignment. Otherwise, the location and the mean

patterns are confounded, which may mislead the alignment operation. Figure 5 shows the alignment of two profiles with and without removing the mean values. It is observed that if the means of the two profiles are not removed first in Figure 4 (a), the latter segment of the query profile is incorrectly mapped to the former segment of the reference profile in Figure 4 (c). But if the means of the two profiles are removed first in Figure 4 (b), then such problem is resolved in Figure 4 (d). Note that the connecting lines between the two profiles in Figure 4 (c) and (d) represent the mapping relationship of the time index.

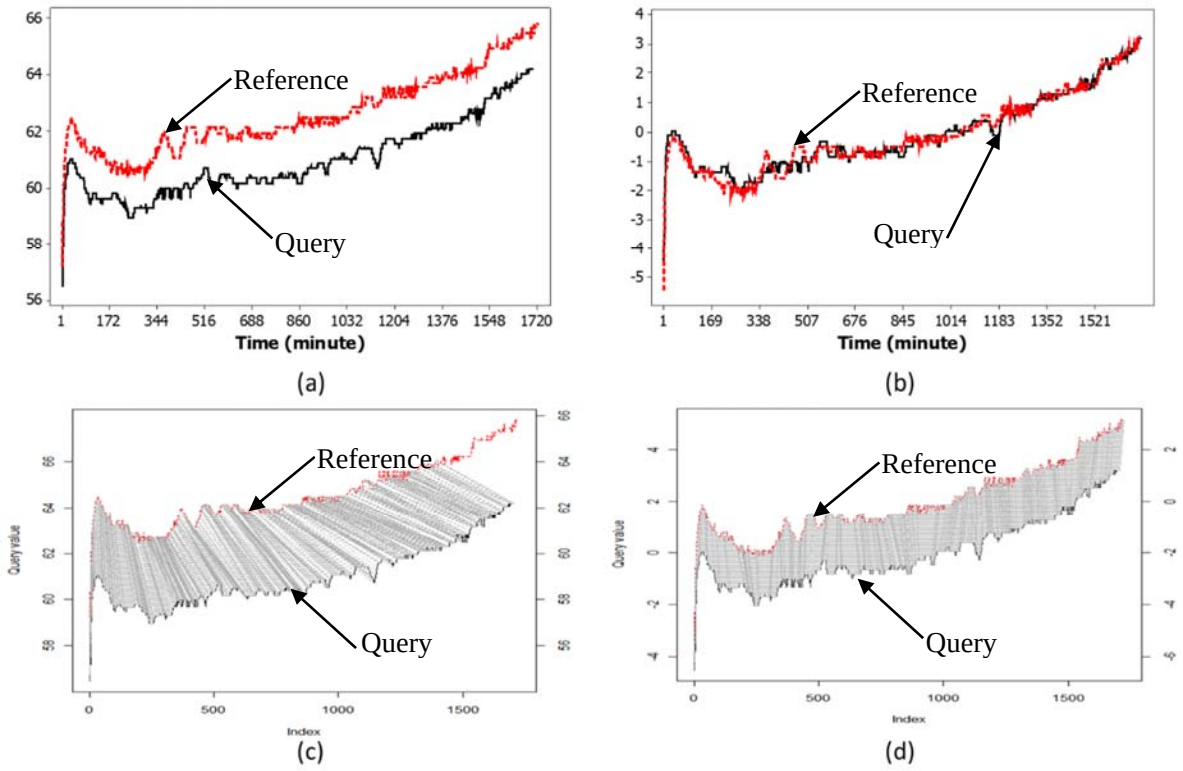

Figure 5. Profile alignment using DTW: (a) two profiles without mean adjustment; (b) two profiles with mean adjustment; (c) alignment of the unadjusted profiles; and (d) alignment of the mean adjusted profiles.

2.2 Baseline profile calculation

Based on a batch of aligned profiles, we will construct a baseline profile for online monitoring. Such baseline profile will identify variation patterns and define an "average" profile from the batch of aligned profiles. The baseline profile is defined as the profile that best captures the variation pattern of multiple profiles. Thus, it can be used as the reference for online comparison and monitoring. Intuitively, the baseline of a collection of profiles can be calculated using an averaging operation. However, the averaging operation is hard to perform if the profiles are not aligned, since they have different lengths in time. Therefore, the aforementioned DTW algorithm is an effective method to make the lengths of different profiles to be the same.

To align multiple profiles, one additional challenge is the selection of the reference profile. Given the reference profile, all other profiles will be treated as queries and mapped to the reference profile. However, a different choice of the reference profile will lead to notably different alignment results. In this paper, we propose an iterative algorithm to identify a reference profile with the minimized total distance.

Algorithm 1. Reference Profile Selection

Denote P_i, $i = 1, ..., N$ are N profiles,

Step 1. Choose P_i as the reference profile, and calculate $D(P_i, P_j)$ as shown in Equation (1) for for all $j \neq i$.

Step 2. Repeat Step 1 for $i = 1, ..., N$. Choose the profile P_i with the $\min_i \sum_{j \neq i} D(P_i, P_j)$ as the reference profile.

For a collection of N profiles, the best choice for the reference profile is the profile that is near the "center" of the samples. In Step 1, all other profiles are adjusted and mapped to P_i. After the

alignment, the total distance of all aligned profiles to P_i is calculated, and this distance is a measure of the deviation of the samples from the reference P_i. In Step 2, we can obtain N deviation measures $D(P_i, P_j)$, $i = 1,...,N$. The profile with the smallest deviation is the closest profile to the "center" of the samples, and it is chosen as the final reference profile for averaging calculation. The search procedure is graphically illustrated in Figure 6.

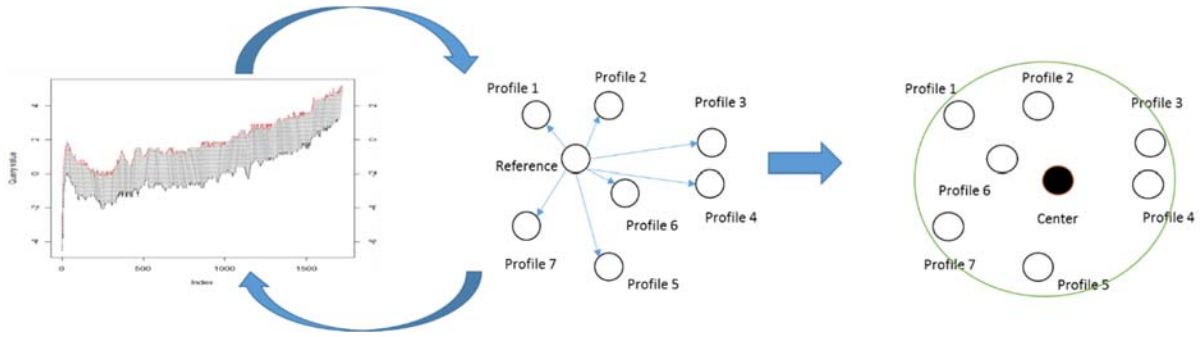

Figure 6. Distance calculation and choice of the reference profile

After the reference profile is identified and all other profiles are registered to it, we have a collection of time-aligned samples. For each time index t, the corresponding mean μ_t and standard deviation σ_t can be calculated from the N aligned profiles. The calculated μ_t will be treated as the baseline profile.

2.3 Online profile alignment and monitoring

In the online growing profile monitoring, we will compare the growing profiles with the baseline profile. Intuitively, an alarm should be triggered if the deviation of the growing profiles from the baseline profile is significant. Because the length of the growing profiles increases with time, time alignment should be performed before online monitoring. In addition, the profiles are always incomplete during online monitoring. Thus, when the query profile (the growing profile)

is being aligned to the reference profile (the baseline profile), we force the query profile and the reference profile to have the same starting time index, but leave the end time index free to move.

Let the growing profile after alignment be y_t, $t = 1,...,n$, and each point y_t follows a normal distribution with an unknown but dynamically changing mean and standard deviation. Because the variation of the in-control samples also varies over time, we calculate the difference between the online profile and the baseline profile, and we standardize it using the time-varying variation:

$$y'_t = (y_t - \mu_t)/\sigma_t . \qquad (2)$$

Hence, all points on the residual profile follow the standard normal distribution $y'_t \sim N(0,1)$. Hawkins *et al.*[22] proposed a generalized likelihood ratio test (GLRT) statistic to detect changes in a process using a change-point model. We apply this method and detect shifts in the residual profile using the following testing statistic:

$$T_{\max,n} = \max_j \left(\sqrt{\frac{j(n-j)}{n}} \frac{\overline{X}_{1j} - \overline{X}_{jn}}{\sigma_{jn}}\right) ,$$

where

$$\overline{X}_{1j} = \sum_{t=1}^{j} y'_t \Big/ j , \ \overline{X}_{jn} = \sum_{t=j+1}^{n} y'_t \Big/ (n-j) , \ \sigma_{jn} = \sqrt{V_{jn}/(n-2)} ,$$

and

$$V_{jn} = \sum_{t=1}^{j} \left(y'_t - \overline{X}_{1j}\right)^2 + \sum_{t=j+1}^{n} \left(y'_t - \overline{X}_{jn}\right)^2 .$$

Hawkins *et al.*[22] suggested that the control limits h_n should be set as the two-sided $\alpha/(n-1)$ fractile of a t-distribution with $n-2$ degrees of freedom, thus to obtain a test with a size of at most α. Therefore, an alarm is triggered in the residual profile if

$$\left|T_{\max,n}\right| > h_n . \tag{2}$$

If the charting statistic exceeds the control limits, we conclude that the process has shifted. When the process evolves, the above testing statistic is evaluated when a new observation becomes available after the time alignment. In this way, the potential process shifts can be detected using the chart with incomplete online profiles. Since this chart is constructed based on the DTW algorithm, we call it the DTW chart.

3 Performance study

In this section, we study the performance of the DTW chart and compare it with another benchmark method. In the literature, there are limited methods that can be directly used to monitor the growing profile that we discuss herein. Zhu *et al.*[23] worked on a similar problem and proposed an adaptive EWMA (AEWMA) chart to monitoring growing profiles. In the following, we briefly introduce the AEWMA chart, then compare our proposed method with it.

The AEWMA chart is modified from existing methods to fit with the time-varying feature of the growing profiles. Capizzi and Masarotto[24] proposed an adaptive EWMA chart to monitor a univariate process with a constant mean. Because the growing profile has a time-dependent mean trend, AEWMA adopts the adaptive EWMA algorithm to capture the dynamic mean trend of the profile as follows:

$$\mu_t = \left(1 - w\left(e_t\right)\right)\mu_{t-1} + w\left(e_t\right) y_t ,$$

where $w\left(e_t\right) = \phi\left(e_t\right)/e_t$ and $e_t = x_t - \mu_{t-1}$ can be considered the prediction error. The weighting function adaptively changes with the prediction error:

$$\phi(e_t)=\begin{cases} e_t+(1-\lambda)k & \text{if } e_t<-k \\ \lambda e_t & \text{if } |e_t|<k \\ e_t-(1-\lambda)k & \text{if } e_t>k \end{cases},$$

where λ is a smoothing parameter and k is determined according to the variation of the profile. If the prediction error is within the range of k, then the adaptive EWMA performs similarly to the conventional EWMA; if the prediction error is larger than k, then the effective smoothing parameter is chosen to be larger than λ. Therefore, it is expected that the AEWMA chart can capture both slow and rapid changes in the growing profile and provide a reasonable smoothing of the profile trend.

The adaptive chart proposed by Capizzi and Masarotto[24] assumes that the variation in the process is fixed. However, the variation in the profile may changes over time in practical problems. Therefore, the AEWMA chart further updates the standard deviation of the profile using a method developed by MacGregor and Harris[25]:

$$\hat{\sigma}_t=\sqrt{(1-\gamma)\hat{\sigma}_{t-1}^2\times+\gamma\left(y_t-\mu_{t-1}\right)^2}\ .$$

where γ is a smoothing parameter that determines how fast the width of the control limits is updated.

Finally, the Shewhart-type AEWMA chart monitors the growing profile as follows

$$\begin{cases} UCL=\mu_t+h*\hat{\sigma}_t \\ CL=\mu_t \\ LCL=\mu_t-h*\hat{\sigma}_t \end{cases}. \qquad (3)$$

3.1 Simulation settings

As previously mentioned, the profiles have certain dynamics, but the trends differ from one profile to another. Thus, we design a two-stage model to simulate the process. The first stage lasts from the first to the $2\pi\ \omega$ minutes to finish a cycle of the sinusoidal function. The model is governed by:

$$y_t = K + a\sin\left(\frac{t}{\omega}\right) + \varepsilon_{1t},\ 0 < t \le 2\pi\ \omega,$$

where $\varepsilon_{1t} \sim N(0, \sigma_t^2)$. The second stage lasts from the $(2\pi\ \omega + 1)$ to the $(2\pi\ \omega + 30/b)$ minutes. The model is governed by:

$$y_t = y_{2\pi\ \omega} + b\left(t - 2\pi\ \omega\right) + \varepsilon_{2t},\quad 2\pi\ \omega < t < 2\pi\ \omega + 30/b\ ,$$

where $\varepsilon_{2t} \sim N\left(0, \sigma_t^2\right)$. In this simulation setting, the overall trends of the profiles can be the same, but the profiles can be misaligned by changing the parameters.

To simulate the misalignment of the profiles, the four parameters K, α, ω and b, are randomly generated from uniform distributions using the values shown in Table 1. To simulate the time-varying variation, the standard deviation σ_t is also a function that changes with t. Figure 7 shows five in-control profiles generated from the above two-stage model. Please note that the profiles are not aligned by default, while such misalignment should not be treated as process failures.

Table 1. Parameter settings to generate historical in-control profiles

Parameters	Effects	Values
K	Position in y-axis	Uniform(0,3)
α	Amplitude of sinusoidal function	Uniform(5,10)
ω	Length in time of the sinusoidal function	Uniform(5,7)
b	Slope of the linear function	Uniform(0.5,1)
σ_t	Standard deviation of the profile	$\sigma_t = e^{-0.01t}$

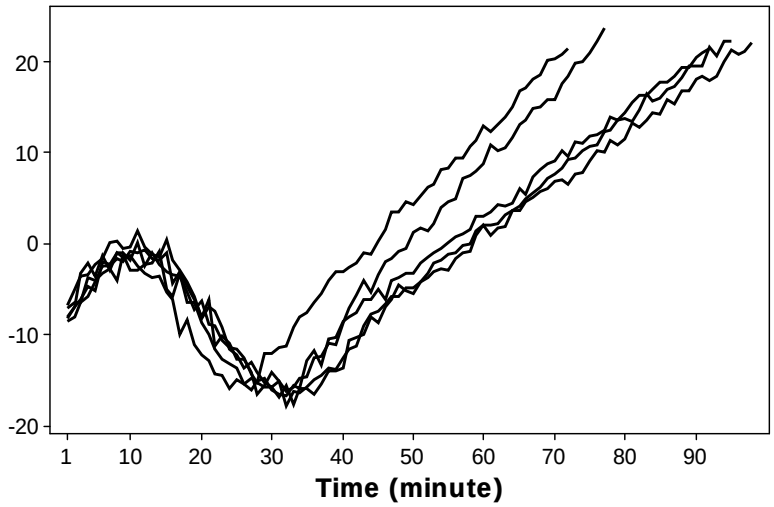

Figure 7. Plots of simulated in-control profiles

In the simulation, we study four types of failure patterns: (1) a sudden mean shift in the second stage after τ_1=35 minutes; (2) a sustained drift in the second stage after τ_2=45 minutes; (3) a constant cyclical shift after τ_1=35 minutes with an added signal $\delta_{t>\tau_1} = A\sin[(t-\tau_1)\pi/\omega]$, which has a fixed magnitude; and (4) a growing cyclical shift after τ_1=35 minutes with an added signal $\delta_{t>K_1} = A\times e^{0.05\times(t-\tau_1)}\times\sin[(t-\tau_1)\pi/\omega]$, which has an increasing amplitude after τ_1=35 minutes. The magnitude of the failure increases step-by-step, as shown in Table 2. The sudden mean shift and the sustained drift are common failure patterns in conventional SPC; the cyclical shifts are used to simulate the dynamic shifts caused by the vibrations of the process, which are commonly observed in complex engineering processes.[26,27]

Table 2. The settings of the failure feature

	Shift pattern	Severity of failure		
Sudden mean shift	$K \to K + \delta_K,\ t > \tau_1$	$\delta_K = 1$	$\delta_K = 5$	$\delta_K = 11$
Sustained drift	$b \to b + \delta_b,\ t > \tau_2$	$\delta_b = 0.2$	$\delta_b = 0.4$	$\delta_b = 0.6$
Constant cyclical shift	$\delta = A\sin[(t-\tau_1)\pi/\omega],\ t > \tau_1$	$A=1, \omega=8$	$A=3, \omega=8$	$A=5, \omega=8$
		$A=3, \omega=2$	$A=3, \omega=4$	$A=3, \omega=16$
Growing cyclical shift	$\delta = Ae^{0.05\times(t-\tau_1)}\sin[(t-\tau_1)\pi/\omega],\ t > \tau_1$	$A=0.3, \omega=8$	$A=0.5, \omega=8$	$A=1.0, \omega=8$

3.2 Control chart implementation

Based on the above models and settings, we implement the proposed DTW chart to monitor the simulated processes, and compare the performance with the AEWMA chart. First, 20 profiles are generated using the parameters given in Table 1 without adding any shifts. Then, these profiles are aligned using DTW; a baseline profile is calculated using the methods introduced in subsections 2.1 and 2.2. Afterward, online profiles are generated step by step. When a new point on the online profile becomes available, the incomplete profile is mapped with respect to the baseline profile using DTW. Then, the aligned profile is standardized using Equation (2). Furthermore, we found that the residual profile has a strong autocorrelation, an AR(1) model is fitted to the residual sequence to remove the autocorrelation. Then, the final uncorrelated residuals are monitored using the chart in Equation (2).

The AEWMA chart defined in Equation (3) is also applied to the same set of simulated profiles for comparison. To make the in-control Average Run Length (ARL) of the two control charts identical, the parameters in the AEWMA chart are set as $\lambda = 0.4$, $\gamma = 0.01$, $k = 1$ and $h = 2.97$.

3.3 Performance comparison

The average run length (ARL) is widely used for evaluating the performance of a control chart. In traditional profile monitoring, each profile is an individual sample, thus the ARL is calculated

as the number of profiles inspected before an alarm is triggered. However, in monitoring growing profiles, the charting statistic is evaluated at each step when a new point on the profile becomes available.

Therefore, here we calculate the average delay in detection, which is defined as the number of steps that a profile runs (counted from the change-point) before an alarm is triggered. If a shift signal is added to the growing profile but an alarm is triggered before the change-point, the alarm is treated as a false alarm. If the profile terminates before an alarm is ever triggered, this sample is removed from calculating either the false alarm rate or the average delay in detection.

To calculate profile-wise charting performance, we simulate 5000 profiles for each shift pattern, then calculate the number of alarms. One a profile triggers an alarm, the process stops.

The simulation results are summarized in Table 3. It is observed that the DTW chart and AEWMA chart have almost equal numbers of alarms when the process is in-control. The AEWMA chart has a smaller average delay in detection than the DTW chart, which implies that more signals on the AEWMA chart occur at the earlier stage of the growing process. For the same reason, when the process becomes out-of-control, we observe that the AEWMA chart has a higher number of false alarms than the DTW chart.

Table 3. Performance comparison

		Number of alarms		Number of false alarms		Average delay in detection	
		DTW	AEWMA	DTW	AEWMA	DTW	AEWMA
In-control		101	99	——		46	25.8
Sudden shift	$\delta_K = 1$	214	243	44	87	24.1	3.5
	$\delta_K = 5$	2956	4975	44	87	4.2	1.6
	$\delta_K = 11$	4968	5000	44	87	1.6	1.0
Sustained drift	$\delta_b = 0.2$	1851	260	50	98	23.3	1.2
	$\delta_b = 0.4$	3238	2115	50	98	11.4	1.1
	$\delta_b = 0.6$	3541	3448	50	98	4.4	1.1
Constant cyclical shift	$A = 1, \omega = 8$	363	168	44	87	24.0	5.3
	$A = 3, \omega = 8$	3239	1898	44	87	16.8	7.2
	$A = 5, \omega = 8$	4836	4190	44	87	11.0	7.5
	$A = 3, \omega = 2$	1612	4454	44	87	17.2	5.4
	$A = 3, \omega = 4$	3830	3190	44	87	10.9	8.5
	$A = 3, \omega = 16$	1438	1816	44	87	21.2	7.3
Growing cyclical shift	$A = 0.3, \omega = 8$	1762	230	44	87	41.6	53.4
	$A = 0.5, \omega = 8$	3258	1393	44	87	37.2	48.8
	$A = 1.0, \omega = 8$	4692	3784	44	87	26.8	35.5

When the process is out-of-control, a number of observations can be made:

(1) When the process has a sudden shift, the AEWMA chart reports more alarms and has a shorter average delay in detection than the DTW chart, which means the AEWMA chart is more powerful for detecting mean shifts.

(2) When the process has sustained shifts, the DTW chart detects more out-of-control profiles than the AEWMA chart. However, because the DTW chart usually requires more observations to make the conclusion, it has a longer average time delay than the AEWMA chart.

(3) For cyclical shifts with a constant amplitude, we can see several trends. For the case with $\omega = 8$, DTW is always better than AEWMA because DTW detects more out-of-control profiles. The detection accuracy also increases when the shift magnitude increases from 1 to 5. However, for the same magnitude $A = 3$, when the frequency of the sinusoidal wave is too high ($\omega = 2$) or too low ($\omega = 16$), the performance of the DTW chart deteriorates. If the frequency is too low, the sine wave has a long cycle, and the failure signal becomes similar to the sustained drift. If the frequency is too high, the DTW alignment may be incorrectly performed, which affects its detection power.

(4) For the cyclical shifts with growing amplitude, the DTW chart is better than the AEWMA chart and also has shorter average time delays in detection. In other words, if the cyclical wave is not mixed with the dynamic variable signal, the DTW chart is more sensitive to these shifts.

In summary, the AEWMA chart is more powerful in detecting mean shift and drifts, while the DTW chart detects cyclical shifts more rapidly. This result can be explained by the fact that the AEWMA chart learns the dynamic profile from its past observations using EWMA smoothing, and a sudden shift or drift signal which cannot be smoothed out by the EWMA smoothing is

easily detected. However, as shown in Figure 5, the DTW chart can be easily distorted by sudden mean shifts. In other words, sudden mean shifts may confound with the increasing trend of the growing profile and mislead the alignment algorithm. However, the DTW alignment algorithm is not affected by the cyclical signal, it is therefore more sensitive to these shifts.

It should be noted that for the same type of shifts, the number of false alarms does not change with the shift magnitude. This result occurs because the false alarms are counted before the shifts are added to the process. Therefore, the shift magnitude does not affect the number of false alarms.

4 A real example in ingot growth processes

In this section, we implement the DTW chart and the AEWMA chart to analyze the heating power profiles from the ingot growth processes, and we demonstrate the use of these charts for real problems.

The dataset was collected during a real ingot growth process. 10 historical conforming profiles are used to estimate the baseline profile for the DTW chart. Both charts are set to have an in-control false alarm rate as 0.01. The parameters used by the AEWMA chart are $\lambda = 0.4$, $\gamma = 0.005$, $k = 0.05$, and $h = 3$. In practice, an autoregressive model is used to remove the autocorrelation in the residual profile before plotting on the control chart. Both charts use the first 15 points to warm-up and start monitoring from the 16^{th} point.

After the control charts are set up, two profiles are tested using the two charts. One profile is considered conforming determined by engineers and the other profile is considered nonconforming, which are shown in Figure 8. It is observed that both charts do not trigger any alarms for the conforming profile. The DTW chart triggers an alarm at Step 145, while the AEWMA chart triggers an alarm at Step 155 for the nonconforming profile.

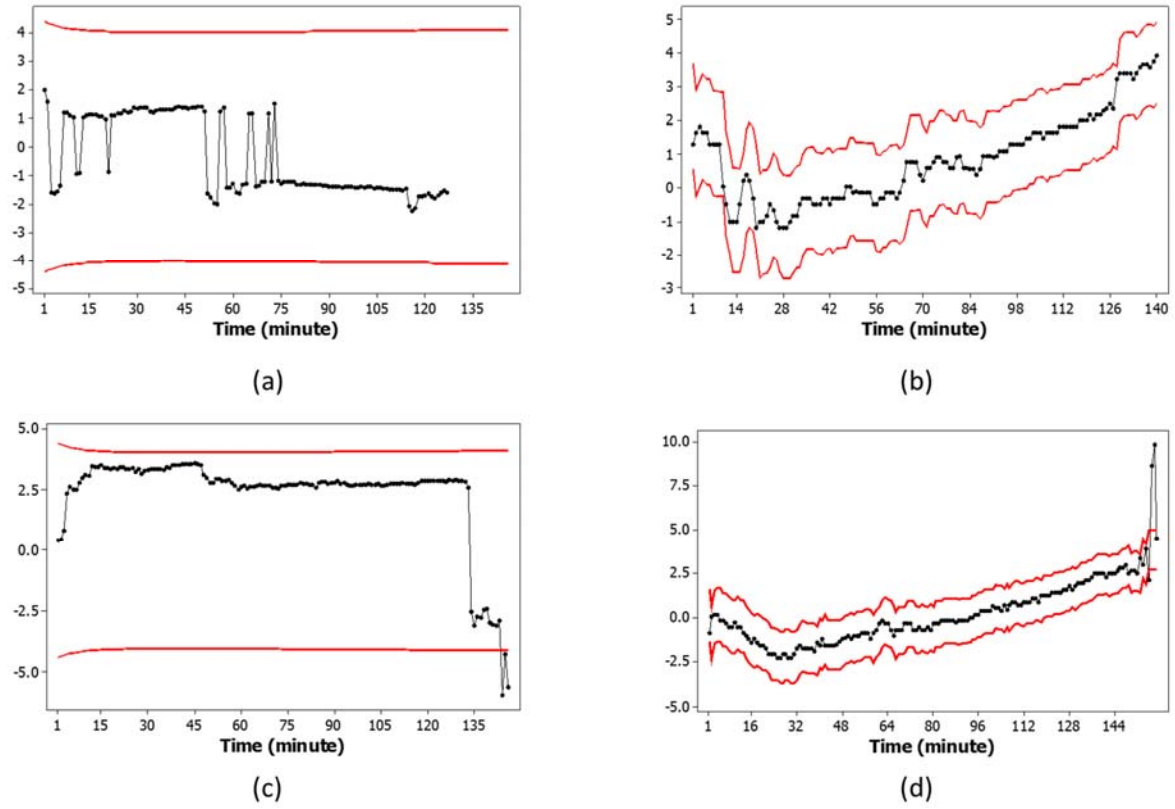

Figure 8. Monitoring of two power profiles: (a) DTW for the in-control profile; (b) AEWMA for the in-control profile; (c) DTW for the out-of-control profile; and (d) AEWMA for the out-of-control profile

5 Conclusions

This paper focuses on the monitoring of growing profiles, which are time dislocated with finite but unequal lengths, and are incomplete during online monitoring. Therefore, the conventional SPC cannot be directly applied for online monitoring.

In this paper, we propose a method for monitoring such growing profiles with DTW based alignment. A baseline profile is calculated from the aligned profiles. During online monitoring, incomplete profiles are aligned with the baseline profile; then the GLRT statistic derived from the change-point theory is evaluated for out-of-control detection. Compared with the modified AEWMA chart, the proposed DTW chart is less sensitive to sudden mean shifts or slow drift, but

it has better performance for detecting cyclical-type dynamic shifts, which are frequently observed in complex engineering processes. Compared with the profiles used in existing research on profile monitoring, the growing profiles that we studied have many unique features, which are both important and challenging. This paper is the first study that addresses the monitoring of growing profiles with time misalignment. It demonstrates the possibility to monitor such profiles based on DTW algorithm.

In future research, we will design new algorithms for alignment considering the practical constraints that apply to real processes. Second, the AEWMA chart learns the growing trend of the process via EWMA smoothing from incomplete online profiles, while the DTW chart learns the trend from historical and completely known profiles. If information from both the historical profiles and the incomplete online profiles are used to predict the growing pattern, we expect that a more accurate result can be obtained. Finally, the real engineering process is characterized by multiple growing profiles, and the monitoring of the process using multiple misaligned profiles is also important for practitioners.

References

1. Stoumbos ZG, Reynolds Jr MR, Ryan TP, Woodall WH. The state of statistical process control as we proceed into the 21st century. *Journal of the American Statistical Association* 2000; **95**: 992-998.
2. Montgomery DC (2005) *Introduction to statistical quality control*. 5th edn. John Wiley, Hoboken, N.J., xvi, 759 p.
3. Woodall WH, Spitzner DJ, Montgomery DC, Gupta S. Using control charts to monitor process and product quality profiles. *Journal of Quality Technology* 2004; **36**: 309-320.
4. Wang K, Tsung F. Using profile monitoring techniques for a data-rich environment with huge sample size. *Quality and Reliability Engineering International* 2005; **21**: 677-688.
5. Williams JD, Woodall WH, Birch JB. Statistical Monitoring of Nonlinear Product and Process Quality Profiles. *Quality and Reliability Engineering International* 2007; **23**: 925-941.
6. Kang L, Albin S. On-line monitoring when the process yields a linear. *Journal of Quality Technology* 2000; **32**: 418-426.

7. Colosimo BM, Semeraro Q, Pacella M. Statistical process control for geometric specifications: on the monitoring of roundness profiles. *Journal of quality technology* 2008; **40**: 1-18.
8. Gardner MM, Lu J-C, Gyurcsik RS, Wortman JJ, Hornung BE, Heinisch HH, Rying EA, Rao S, Davis JC, Mozumder PK. Equipment fault detection using spatial signatures. *IEEE Transactions on Components, Packaging, and Manufacturing Technology - Part C* 1997; **20**: 295-304.
9. Jones M, Rice JA. Displaying the important features of large collections of similar curves. *The American Statistician* 1992; **46**: 140-145.
10. Nomikos P, MacGregor JF. Multivariate SPC charts for monitoring batch processes. *Technometrics* 1995; **37**: 41-59.
11. Jeong MK, Lu J-C, Huo X, Vidakovic B, Chen D. Wavelet-based data reduction techniques for process fault detection. *Technometrics* 2006; **48**.
12. Walker E, Wright SP. Comparing curves using additive models. *Journal of Quality Technology* 2002; **34**: 118-129.
13. Zou CL, Tsung FG, Wang ZJ. Monitoring Profiles Based on Nonparametric Regression Methods. *Technometrics* 2008; **50**: 512-526.
14. Del Castillo E, Colosimo BM. Statistical shape analysis of experiments for manufacturing processes. *Technometrics* 2011; **53**: 1-15.
15. Wright CM, Booth DE, Hu MY. Joint estimation: SPC method for short-run autocorrelated data. *Journal of Quality Technology* 2001; **33**: 365-378.
16. Zantek PF, Wright GP, Plante RD. A self-starting procedure for monitoring process quality in multistage manufacturing systems. *IIE Transactions* 2006; **38**: 293-308.
17. Myers C, Rabiner L. A comparative study of several dynamic time-warping algorithms for connected word recognition. *The Bell System Technical Journal* 1981; **60**: 1389-1409.
18. Giorgino T. Computing and visualizing dynamic time warping alignments in R: the dtw package. *Journal of Statistical Software* 2009; **31**: 1-24.
19. Gupta A, Samanta A, Kulkarni B, Jayaraman V (2007) Fault diagnosis using dynamic time warping. *Pattern Recognition and Machine Intelligence*. Springer, 57-66.
20. Dai Y, Zhao J. Fault Diagnosis of Batch Chemical Processes Using a Dynamic Time Warping (DTW)-Based Artificial Immune System. *Industrial & Engineering Chemistry Research* 2011; **50**: 4534-4544.
21. Kassidas A, MacGregor JF, Taylor PA. Synchronization of batch trajectories using dynamic time warping. *AIChE Journal* 1998; **44**: 864-875.
22. Hawkins DM, Qiu PH, Kang CW. The changepoint model for statistical process control. *Journal of Quality Technology* 2003; **35**: 355-366.
23. Zhu L, Li W, Dai C, Sun H, Wang K, Jin R. Growing Curve Monitoring for a Single-Crystal Ingot Growth Process. *Submitted* 2013.

24. Capizzi G, Masarotto G. An adaptive exponentially weighted moving average control chart. *Technometrics* 2003; **45**: 199-207.
25. MacGregor J, Harris T. The exponentially weighted moving variance. *Journal of Quality Technology* 1993; **25**.
26. Wang K, Tsung F. Monitoring feedback-controlled processes using adaptive T2 schemes. *International Journal of Production Research* 2007; **45**: 5601-5619.
27. Wang K, Tsung F. An adaptive T^2 chart for Monitoring Dynamic Systems. *Journal of Quality Technology* 2008; **40**: 109-123.